

# Low-Pressure Synthesis and Characterization of Hydrogen-Filled Ice Ic\*\*

Rajnish Kumar, Dennis D. Klug, Christopher I. Ratcliffe, Christopher A. Tulk, and John A. Ripmeester\*

The discovery of a hydrogen clathrate<sup>[1]</sup> in 2002, formed at about 200 MPa, led to suggestions for its use for hydrogen storage from its maximum hydrogen storage capacity<sup>[2]</sup> of 3.9 wt %. This material would seem to be an ideal storage medium as it contains only hydrogen and water. It has the same structure as that found for many other clathrate hydrates, with molecular or atomic guests enclosed in cages formed by hydrogen-bonded water molecules, known as structure II (Str. II) clathrate hydrate.<sup>[3]</sup> For practical hydrogen storage applications however, there is the need to find pressures lower than the 200 MPa required for the preparation of Str. II hydrogen hydrate without significantly lowering the maximum storage capacity. The motivation for this study was to find a gentle method for the synthesis of Str. II hydrogen hydrate. According to the *P-T* phase diagram, it should be possible to use low pressures at low temperatures. However, pressurizing the normal ice Ih phase at low temperatures produces little or no conversion on a practical time scale. One approach would be to find more reactive forms of ice. For instance, a low-density amorphous ice phase can be prepared at low temperatures.<sup>[4]</sup> Exposure to a hydrogen pressure at sufficient pressure and upon annealing at somewhat higher temperatures, the metastable amorphous phase plus gas should convert to a crystalline phase (e.g. a clathrate<sup>[5,6]</sup>) under temperature control of the conversion kinetics. This approach indeed produced small amounts of Str. II clathrate hydrate in some preparations. However, the main product proved to be an even more interesting material.

We demonstrate that amorphous ice plus hydrogen gas can be converted to an ice Ic framework partially filled with H<sub>2</sub> (designated as H<sub>2</sub>:H<sub>2</sub>O-Ic), by annealing at pressures less than 18 MPa. This material is stable at ambient pressure at

77 K. From calculations, we suggest that it may be possible to prepare 50 % filled H<sub>2</sub>:H<sub>2</sub>O-Ic (5.3 wt % H<sub>2</sub>) at pressures below 45 MPa. This material may be closely related to the C<sub>2</sub> structure stable at 3 GPa<sup>[7,8]</sup> and could have broad implications for hydrogen storage and also astrophysics. Indeed it may be present in our solar system and elsewhere, wherever vapor deposition and annealing are common processes.

Powder X-ray diffraction patterns obtained at 130 K (Figure 1) show that a) the vapor-deposited H<sub>2</sub>O or D<sub>2</sub>O used as the starting material was low-density amorphous ice with detectable traces of crystalline ice;<sup>[9]</sup> b) the material recovered at ambient pressure, after annealing amorphous ice between 140–160 K under a pressure of H<sub>2</sub> or D<sub>2</sub>, is mainly ice Ic with stacking faults<sup>[10–12]</sup> and a slightly enlarged unit cell compared to ice Ic. No reflections of the Str. II clathrate hydrate were observed in the PXRD samples.

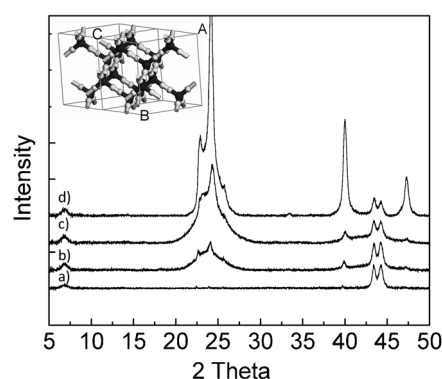


**Figure 1.** Powder X-ray diffraction data for amorphous ice and annealed amorphous ice after filling with hydrogen gas at 77 K. a) Sample holder, b) amorphous ice from vapor deposition at 15 K, stored in liquid nitrogen and analyzed at 120 K, showing traces of ice Ic and ice Ih. c) Sample prepared from amorphous ice with 15 MPa H<sub>2</sub> and 140 K annealing, then analyzed at 130 K, showing a mixture of ice Ic, and amorphous ice. d) Ice Ic sample prepared from amorphous ice with 15 MPa H<sub>2</sub> and 150 K annealing, then analyzed at 130 K.

Raman spectra (Figure 2) provide some of the key evidence that H<sub>2</sub> or D<sub>2</sub> is incorporated in the ice Ic formed: The H<sub>2</sub> vibron spectrum (Figure 2a) is uniquely different from that of Str. II hydrogen hydrate with a broad asymmetric peak at about 4126 cm<sup>-1</sup> for H<sub>2</sub>:H<sub>2</sub>O-Ic and H<sub>2</sub>:D<sub>2</sub>O-Ic, 27 cm<sup>-1</sup> lower than the 4155.2 cm<sup>-1</sup> Q<sub>1</sub>(1) band of ambient pressure gaseous H<sub>2</sub><sup>[13]</sup> (likewise, 2977 cm<sup>-1</sup> for D<sub>2</sub>:D<sub>2</sub>O-Ic versus 2991.4 cm<sup>-1</sup> for D<sub>2</sub> gas). The frequencies are also lower than in pure solid H<sub>2</sub> (about 4150 cm<sup>-1</sup>) and D<sub>2</sub> (about 2984 cm<sup>-1</sup>),<sup>[14]</sup> H<sub>2</sub> in a dense ice<sup>[8]</sup> at 2.3 GPa (about

[\*] Dr. D. D. Klug, Dr. C. I. Ratcliffe, Dr. J. A. Ripmeester  
National Research Council of Canada  
100 Sussex Dr., Ottawa, ON, K1A0R6 (Canada)  
E-mail: john.ripmeester@nrc-cnrc.gc.ca

Dr. R. Kumar  
Chemical Engineering and Process Development Division  
CSIR—National Chemical Laboratory, Pune, 411008 (India)

Dr. C. A. Tulk  
Neutron Scattering Science Division, Oak Ridge National Laboratory  
Oak Ridge, TN 37831 (USA)

[\*\*] A part of this research at ORNL's Spallation Neutron Source was sponsored by the Scientific User Facilities Division, Office of Basic Energy Sciences, U.S. Department of Energy. The authors also thank G. McLaurin and S. Lang for technical assistance.

Supporting information for this article is available on the WWW under <http://dx.doi.org/10.1002/anie.201208367>.

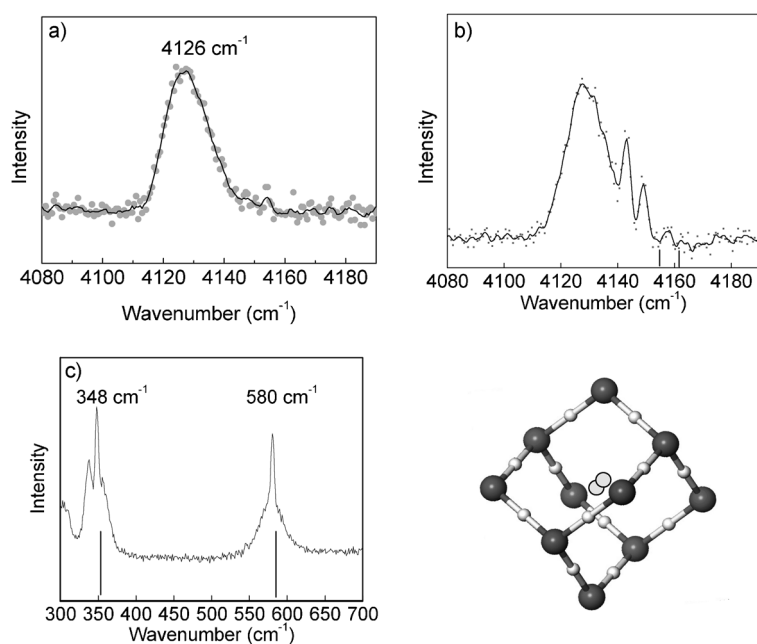


**Figure 2.** Raman spectra at ambient pressure and 77 K of samples prepared by annealing amorphous ice at 140 K exposed to  $H_2$  at pressures of 15 or 18 MPa. a)  $H_2$  vibron band of  $H_2:H_2O$ -Ic. b)  $H_2$  vibron band of  $H_2:H_2O$ -Ic showing additional sharp lines from  $H_2$  Str. II clathrate hydrate and vertical lines for  $H_2$  gas-phase vibron frequencies.<sup>[13]</sup> c)  $H_2$  roton bands showing sharper  $H_2$  Str. II clathrate hydrate lines superimposed on broader  $H_2:H_2O$ -Ic bands (*para*- $H_2$  band at lower frequency). d)  $H_2$  molecule at the center of an adamantane-shaped cavity in ice Ic.

4150  $cm^{-1}$ ) and  $H_2$  in ice Ih (about 4173  $cm^{-1}$ ).<sup>[15]</sup> However, Str. II  $H_2$  clathrate hydrates show narrow, multiple peaks in the same region,<sup>[16–18]</sup> which are assigned to *ortho*- $H_2$  and *para*- $H_2$  in small and large cages with different occupancies. The broadening and lack of *ortho*- $H_2$  and *para*- $H_2$  resolution in the  $H_2:H_2O$ -Ic spectrum was attributed to a distribution of  $H_2$  environments in the ice Ic lattice arising from defects and the inherent stacking faults.<sup>[10–12]</sup> Notwithstanding the above observations, in a few preparations two sharp lines appeared at about 4144 and about 4150  $cm^{-1}$  on top of the broad spectrum (Figure 2b). These correspond well to the *ortho*- $H_2$  and *para*- $H_2$  peaks assigned to 4  $H_2$  in the large cage of Str. II clathrate hydrate.<sup>[17]</sup> Figure 2c displays two  $H_2$  roton bands centered at about 580 and 348  $cm^{-1}$  corresponding to *ortho*- $H_2$   $S_0(1)$  and *para*- $H_2$   $S_0(0)$ , which are again significantly broader than the weak, superimposed Str. II  $H_2$  clathrate hydrate lines.<sup>[16,17]</sup>

In situ neutron diffraction data obtained on amorphous ice, pressurized under  $D_2$  gas followed by annealing, revealed the structural evolution from amorphous ice to ice Ic. Figure 3 shows diffraction data during annealing at 140 and 150 K, and upon quenching (see also Figure S1 in the Supporting Information), and indicates the formation of some Str. II hydrate that could also be an intermediate form prior to formation of ice Ic. The indicated peaks are consistent with the presence of a Str. II clathrate hydrate and in agreement with Raman scattering data. This intermediary largely disappears after pumping away the  $D_2$  gas, but some remnants are observed even after formation of ice Ic. Another amor-

phous  $D_2O$  sample, after annealing under  $H_2$  pressure to form ice Ic, showed increased incoherent scattering from  $H_2$ . A comparison of the experimental radial distribution function  $G(R)$  from neutron scattering data (Figure 2S) with the  $G(R)$  calculated for ideal ice Ic by molecular dynamics (MD) employing the Faber–Ziman approximation,<sup>[19]</sup> indicates that stacking faults, which significantly perturb the X-ray diffraction patterns of ice Ic, have very little effect on the  $G(R)$ .

Ice Ic has adamantane-shaped cavities, and partial radial distribution functions,  $G(R)$ , obtained from MD simulations up to 1  $H_2:1 H_2O$  loading, show that the mean position of  $H_2$  is at the center of these cavities. MD also showed about 2% increase in the lattice volume at 1  $H_2:8 H_2O$  loading, consistent with the expansion observed by diffraction techniques.

Static solid-state  $^1H$  and  $^2H$  NMR spectra, Figure 4, provide unambiguous confirmation of the presence of hydrogen in these ice Ic materials: 1) The broad  $^1H$  spectrum for  $H_2:D_2O$ -Ic (linewidth 36 kHz) indicates that  $H_2$  is contained in a solid phase, the lineshape arising predominantly from  $^1H$ - $^1H$  dipolar coupling between  $H_2$  molecules in adjacent cavities. This linewidth is greater than that observed at 77 K for  $H_2$  in the cages of Str. II  $D_2O$  clathrate hydrate (11.6 kHz),<sup>[20]</sup> consistent

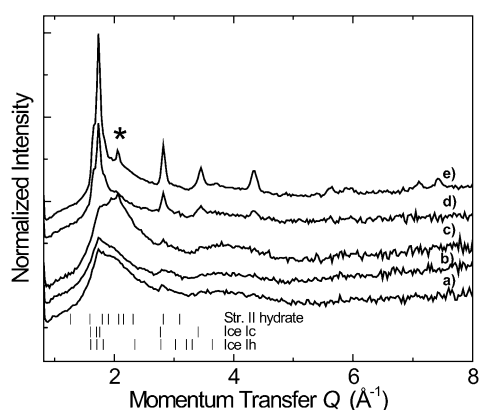


**Figure 3.** In situ neutron diffraction data for annealing of amorphous ice under a  $D_2$  gas pressure of 11.7 MPa, sequentially from bottom: a) not annealed, b) annealed at 140 K, c) quenched to 50 K, d) annealed at 150 K, and e) quenched to 50 K. The vertical lines identify the location of the features due to ice phases and Str. II clathrate hydrate. The dominant peak of the Str. II clathrate is indicated by the “\*”.

with a shorter distance and stronger dipolar coupling between  $H_2$  molecules: 2.75 Å between cavity centers in ice Ic versus 6.12 to 7.18 Å in the hydrate.<sup>[2,21,22]</sup> 2) The broadening of the  $^1H$  spectrum of  $H_2:H_2O$ -Ic (linewidth 88 kHz) compared to empty ice Ic (linewidth 68.1 kHz<sup>[23]</sup>), arises from additional  $^1H$ - $^1H$  dipolar couplings between  $H_2$  molecules in adjacent cavities and between  $H_2$  and  $H_2O$ . 3) The dynamics of the  $H_2$

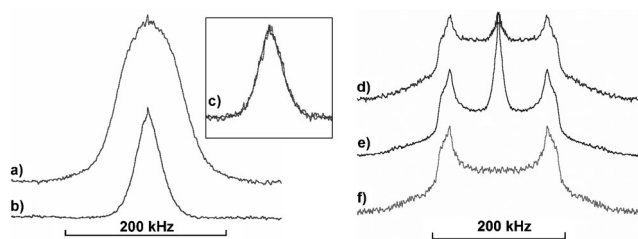


**Figure 4.** Left:  $^1\text{H}$  NMR spectra (300 MHz) at 77 K: a)  $\text{H}_2\text{:H}_2\text{O-Ic}$  (prepared at 17.5 MPa, 150 K) and b)  $\text{H}_2\text{:D}_2\text{O-Ic}$  (13.5 MPa, 150 K). Recycle times of 1 s. Spectra scaled to show approximate relative intensities. c) Two superimposed spectra of  $\text{H}_2\text{:D}_2\text{O-Ic}$  with different recycle times. 400 scans at 1 s per scan, 40 scans at 30 s per scan and scaled up by a factor of 10. Right:  $^2\text{H}$  NMR spectra (46.05 MHz) at 77 K: d,e)  $\text{D}_2\text{:D}_2\text{O-Ic}$  (16 MPa, 150 K), recycle times of 300 s and 8 s respectively and f)  $\text{D}_2\text{O}$  amorphous ice after pressurizing with  $\text{D}_2$  at 10 MPa, annealing at 110 K, and depressurizing at a recycle time of 300 s.

molecules also drastically reduce the spin–lattice relaxation time ( $T_1$ ) from about 7300 s for empty ice Ic<sup>[24]</sup> to less than 1 s for  $\text{H}_2\text{:H}_2\text{O-Ic}$  and  $\text{H}_2\text{:D}_2\text{O-Ic}$ . 4)  $^1\text{H}$  NMR spectroscopy of  $\text{D}_2\text{:D}_2\text{O-Ic}$  shows a broad lineshape because of static  $\text{D}_2\text{O}$  and a narrow and more rapidly relaxing lineshape due to dynamic  $\text{D}_2$ . In contrast, a sample prepared in the same way but annealed at only 110 K (hence no conversion of amorphous ice to  $\text{D}_2\text{:D}_2\text{O-Ic}$ ) shows no  $\text{D}_2$  signal in the  $^2\text{H}$  NMR spectrum, indicating no retention of  $\text{D}_2$  by amorphous ice at 77 K and ambient pressure. A particularly interesting observation is the surprising stability of  $^2\text{H}\text{:H}_2\text{O-Ic}$ : NMR spectra for two samples stored at 77 K showed that 40–50 % of their original  $\text{H}_2/\text{D}_2$  loading are still present after 27 months. The  $\text{H}_2\text{:H}_2\text{O-Ic}$  stability is most likely due to the smaller, less regular channels in ice Ic compared to ice Ih, and the stacking faults in ice Ic.

The potentially large  $\text{H}_2$  capacity of ice Ic (10 wt % if fully loaded) prepared by this route at moderate pressures suggests ice Ic could be a viable hydrogen storage material. A crude estimate of the level of  $\text{H}_2$  loading achieved in our experiments, based on the relative intensities of the  $^1\text{H}$  NMR spectra of Figure 4 a,b, suggests a 20–30 % loading, assuming various factors remain constant between samples. Since this was achieved at hydrogen pressures of 15–18 MPa, significantly higher occupancy might be achieved at higher but still moderate pressures. This contrasts with the about 200 MPa required to form pure hydrogen clathrate hydrate (about 3.9 wt %) at 295 K.<sup>[3]</sup> Table 1 gives calculated  $\text{H}_2$  gas pressures equivalent to the  $\text{H}_2$  density at several loadings in the ice Ic lattice, taking into account nonideal behavior with 2nd and 3rd virial coefficients<sup>[25]</sup> at the volume of ice Ic at 80 K.<sup>[22]</sup> We regard these as maximum pressures for stability since, as shown in a recent computational study of  $\text{H}_2$  in ice Ih,<sup>[26]</sup> there

will also be a binding energy associated with inclusion in the cavity that should reduce the pressure requirements.

For 0.25  $\text{H}_2\text{:H}_2\text{O}$  corresponding to 2.7 wt %, the  $\text{H}_2$  density is equivalent to  $\text{H}_2$  gas at 17.2 MPa at 140 K, a value comparable to pressures used in our preparations. We note that for most hydrogen storage materials, considerable mass remains after  $\text{H}_2$  is released. In contrast, there is no residual mass if water produced from  $\text{H}_2/\text{ice Ic}$  is expelled as liquid or vapor.

The ice Ic framework  $\text{H}_2\text{:H}_2\text{O-Ic}$  may be related to the reported high-pressure  $\text{C}_2$  structure,<sup>[7,8,27,28]</sup> in which hydrogen molecules may occupy sites remaining when one of the interpenetrating Ic lattices forming ice VII or VIII is removed, resulting in a 1:1  $\text{H}_2/\text{H}_2\text{O}$  composition. However, none of the H atom positions have yet been unambiguously determined. In a recent study<sup>[27]</sup> it was suggested that, on decompression,  $\text{C}_2$  transforms to empty ice Ic at 110 K and 0.3 GPa. However, the present results suggest that this might not be empty, and consequently we suggest that the  $\text{C}_2$  phase might have a  $\text{H}_2\text{:H}_2\text{O}$  ratio greater than 1 and the reported transition instead represents partial loss of  $\text{H}_2$  to a filled or partially filled ice Ic.

In summary, in this low-temperature approach a combination of factors results in the incorporation of  $\text{H}_2$  into the ice Ic (or in some cases the Str. II clathrate hydrate) framework upon annealing: The exceptional porosity of vapor-deposited amorphous ice<sup>[29]</sup> allows intimate contact between ice and  $\text{H}_2$  over a very large surface area throughout the material, and moderate pressures make a high concentration of  $\text{H}_2$  available right at the sites where reorganization of low-density amorphous ice into ice Ic occurs following the apparent glass transition at about 135 K, ensuring efficient  $\text{H}_2$  incorporation into the ice Ic cavities. The general principle illustrated is that the use of a metastable form of ice allows control of the kinetics of transformation to a crystalline phase with temperature. Here, the unexpected result was the appearance of an unusual phase, again adding to our knowledge of the complex phase equilibria of icy materials.

## Experimental Section

Amorphous  $\text{H}_2\text{O}$  and  $\text{D}_2\text{O}$  ices were prepared at the National Research Council of Canada (NRC) Steacie Institute for Molecular Sciences by vapor deposition of water vapor onto a copper cold plate in a vacuum chamber on the evacuated tail of a DISPLEX closed-cycle helium cryostat maintained at 20 K. Depositions of two to three grams of amorphous ice were made over a 24 hour period. Samples were then removed at 77 K and stored in liquid nitrogen until used for further sample characterization and subsequent sample preparations. The amorphous ice was placed in high-pressure Swagelok stainless steel vessels cooled with liquid nitrogen which were then warmed to 80 K and evacuated to remove residual nitrogen gas. The vessel was then filled with cold hydrogen or deuterium gas and the amorphous ice plus hydrogen was then annealed to temperatures in the range 135–160 K. The hydrogen gas pressure was typically between 8–18 MPa. After annealing, samples were recooled to 77 K, removed from the pressure vessel and maintained at 77 K before characterization by NMR spectroscopy, neutron and X-ray powder diffraction, and Raman spectroscopy. Details of the characterization and

**Table 1:** Equivalent  $\text{H}_2$  gas pressures  $P$  in [MPa].

$\text{H}_2\text{:H}_2\text{O-Ic}$	$\text{H}_2$ capacity [wt %]	$P(77\text{ K})$	$P(140\text{ K})$	$P(150\text{ K})$
1:1	10	76.0	161.0	174.2
0.5:1	5.263	19.4	44.4	48.3
0.25:1	2.703	7.9	17.2	18.6

molecular dynamics calculation methods can be found in the Supporting Information.

Received: October 17, 2012

Published online: December 21, 2012

**Keywords:** clathrates · cubic ice · hydrates · hydrogen

- [1] W. L. Mao, H. K. Mao, A. F. Goncharov, V. V. Struzhkin, Q. Guo, J. Hu, J. Shu, R. J. Hemley, M. Somayazulu, Y. Zhao, *Science* **2002**, 297, 2247–2249.
- [2] Y. Zhao, D. He, W. L. Mao, H. K. Mao, R. J. Hemley, *Phys. Rev. Lett.* **2004**, 93, 125503.
- [3] T. C. W. Mak, R. K. McMullan, *J. Chem. Phys.* **1965**, 42, 2732–2737.
- [4] E. Mayer, R. Pletzer, *J. Chem. Phys.* **1984**, 80, 2939–2952.
- [5] A. Hallbrucker, E. Mayer, *J. Chem. Soc. Faraday Trans.* **1990**, 86, 3785–3792.
- [6] J. A. Ripmeester, L. Ding, D. D. Klug, *J. Phys. Chem.* **1996**, 100, 13330–13332.
- [7] W. L. Vos, L. W. Finger, R. J. Hemley, H. K. Mao, *Phys. Rev. Lett.* **1993**, 71, 3150.
- [8] W. L. Vos, L. W. Finger, R. J. Hemley, H. K. Mao, *Chem. Phys. Lett.* **1996**, 257, 524–530.
- [9] A. Hallbrucker, E. Mayer, *J. Phys. Chem.* **1989**, 93, 4986–4990.
- [10] W. F. Kuhs, D. V. Bliss, J. L. Finney, *J. Phys.* **1987**, 48, C1631–636.
- [11] T. C. Hansen, M. M. Koza, W. F. Kuhs, *J. Phys. Condens. Matter* **2008**, 20, 285104.
- [12] T. C. Hansen, M. M. Koza, P. Lindner, W. F. Kuhs, *J. Phys. Condens. Matter* **2008**, 20, 285105.
- [13] B. P. Stoicheff, *Can. J. Phys.* **1957**, 35, 730–741.
- [14] S. S. Bhatnagar, E. J. Allin, H. L. Welsh, *Can. J. Phys.* **1962**, 40, 9–23.
- [15] D. G. Taylor III, H. L. Strauss, *J. Chem. Phys.* **1992**, 96, 3367–3369.
- [16] A. Giannasi, M. Celli, L. Ulivi, M. Zoppi, *J. Chem. Phys.* **2008**, 129, 084705.
- [17] T. A. Strobel, E. D. Sloan, C. J. Koh, *J. Chem. Phys.* **2009**, 130, 14506.
- [18] H. Lu, J. Wang, C. Liu, C. I. Ratcliffe, U. Becker, R. Kumar, J. A. Ripmeester, *J. Am. Chem. Soc.* **2012**, 134, 9160–9162.
- [19] T. E. Faber, J. M. Ziman, *Philos. Mag.* **1965**, 11, 153–173.
- [20] L. Senadheera, M. S. Conradi, *J. Phys. Chem. B* **2007**, 111, 12097–12102.
- [21] Intercavity distances were derived from crystal structures of Str. II hydrate<sup>[3]</sup> and ice Ic<sup>[22]</sup>.
- [22] G. P. Arnold, E. D. Finch, S. W. Rabideau, R. G. Wenzel, *J. Chem. Phys.* **1968**, 49, 4365–4369.
- [23] S. W. Rabideau, E. D. Finch, A. B. Denison, *J. Chem. Phys.* **1968**, 49, 4660–4665.
- [24] J. A. Ripmeester, C. I. Ratcliffe, D. D. Klug, *J. Chem. Phys.* **1992**, 96, 8503–8508.
- [25] R. D. Goodwin, D. E. Diller, H. M. Roder, L. A. Weber, *J. Res. Natl. Bur. Stand. Sect. A* **1964**, 68, 121–126.
- [26] T. A. Pascal, C. Boxe, W. A. Goddard III, *J. Phys. Chem. Lett.* **2011**, 2, 1417–1420.
- [27] T. A. Strobel, M. Somayazulu, R. J. Hemley, *J. Phys. Chem. C* **2011**, 115, 4898–4903.
- [28] S. Machida, H. Hirai, T. Kawamura, Y. Yamamoto, T. Yagi, *J. Phys. Conf. Ser.* **2010**, 215, 012060.
- [29] E. Mayer, R. Pletzer, *Nature* **1986**, 319, 298–301.